Journal Homepage: -www.journalijar.com
INTERNATIONAL JOURNAL OF ADVANCED RESEARCH (IJAR)
Article DOI:10.21474/IJAR01/1501
DOI URL: http://dx.doi.org/10.21474/IJAR01/1501
ISSN NO. 2320-5407

RESEARCH ARTICLE

SYNTHESIS AND CHARACTERIZATION OF Fe, Mn AND SUPER PARAMAGNETIC MAGNETITE Fe_3O_4 NANOPARTICLES.

Mostafa M. Emara[1], Mohamed E Goher[2], Mohamed H Abdo[2], Nesrine M.Mahmod[3] and Amr S. El-Shamy[2].

1. Department of chemistry, Faculty of science, Al-Azharuniversity, Cairo, Egypt.
2. Laboratory of chemistry, Freshwater and lakes division, National Institute of Oceanography, Fisheries (NIOF), Cairo, Egypt.
3. Department of chemistry, Faculty of pharmacy, Al-Nahdauniversity, BaniSwaif, Egypt.

Manuscript Info

Manuscript History

Received: 16 July 2016
Final Accepted: 19 August 2016
Published: September 2016

Key words:-
Ion exchange polymer, Magnetite, Nanowafer, FeNPs, MnNPs, SPMM Fe_3O_4 NWNPs.

Abstract

Ion exchange polymer is a matrix normally insoluble and in the form of small beads having diameters of 300 - 1200 µm, fabricated from organic substrates. This paper deal with three different types of strong acid cation exchanger resins (PUROLITE C-145, DOSHIONCSA 29 and AMBERLIT IR 120 H resin), which have highly developed structure of pores on the surface and the framework contains some active sites. Active sites of strong acid cation exchanger resins are generally charged with H^+ or Na^+.The previous three strong acid cation exchanger resins are used as support through the simple chemical–thermal technique.to produce a hybrid spherical macro porous polymeric cation exchanger beads within which HMO (where M=Fe &Mn) particles (Fe, Mnandsuper paramagnetic magnetite Fe_3O_4NanowafersNanoparticles (SPMM Fe_3O_4 NWNPs). To characterize thesize, shape and strong magnetic of magnetite, porous of these Nanoparticles using Scanning Electron Microscopy (SEM), X-ray Diffraction (XRD) and Fourier Transform Infrared spectroscopy (FTIR), Magnetic Susceptibility Balance (MSB).The average particle size of Nanoparticles was calculated from the XRD study. The average particle size of Fe NPs was 2.3-6.6 nm, MnNPs was 2.6-65.5 nm and Fe_3O_4NPs (DOSHIONCSA 29) was 16-56.5 nm,Fe_3O_4NPs (AMBERLIT IR 120 H) was 2.9-33.2 nm. Their unique properties make it possible to envision a series of in partial or complete removal of hazardous pollutants in industrial wastewater, which will be published in a follow up publications.

Copy Right, IJAR, 2016,. All rights reserved.

Introduction:-

Nano scale materials are defined as a set of substances where at least one dimension is less than approximately 100 nanometers. A nanometer is one millionth of a millimeter approximately 100,000 times smaller than the diameter of a human hair (Alagarasi, 2013). Nanotechnology primarily deals with the synthesis, characterization, exploration and exploitation of nanostructured materials. These materials are characterized by at least one dimension in the nanometer (1nm = 10^{-9} m) range (Gogotsi, 2006). NPs can be synthesized by different approaches. Generally, Nanoparticle production can categorize the synthesis processes according to the different mechanisms responsible

Corresponding Author: - Amr S. El-Shamy.
Address: -Laboratory of Chemistry, Freshwater and lakes division, National Institute of Oceanography, Fisheries (NIOF), Cairo, Egypt. E-mail: amrsalah1980@gmail.com

for their formation (Aitken et al., 2004; BSI, 2005). Some studies prefer to divided the synthesis processes into three major categories based on the approaches used (synthesized Nanoparticle) chemical processes, physical processes and mechanical processes (Emaraet al., 2010). Prefers to describe the different synthesis processes by major nanoparticle class. (ICON 2008). Several methods have been reported for the preparation of polymer-based inorganic NPs composites. The most important are: (i) intercalation of NPs with the polymer or pre-polymer from solution (Alexandre, Dubois, 2000); (ii) In sit intercalative polymerization (Okamoto et al., 2000); (iii) Melt intercalation (Vaia, Giannelis, 1997); (iv) Direct mixture of polymer and particulates (Gyooet al., 2006); (v) Template synthesis (Tomaskoet al., 2003); (vi) In sit polymerization (Aymonieret al., 2003) and (vii) sol-gel process (Kickelbick, 2003).Publications dealing with various methods for the incorporation of NPs into conducting polymers are also available. The most prominent one is probably the incorporation of inorganic NPs in polymers (El-Moselhyet al., 2014). Polymer based Nano composite synthesis was affected by molecular weight, inorganic particles size and content, properties of inorganic particles (In-Yup, Jong-Beom, 2010). Synthesis of metal NPs on a resin surface having a charge on it can serve all these purpose satisfactorily (Chauhan, 2011). Ion exchange resinsare widely used in different separation, purification, and decontamination processes. The most common examples are water softening and water purification. In many cases, resins consisting of polystyrene with sulfonate groups to form cation exchangers (Emaraet al., 2010). The affinity of sulfonic acid resins for cations varies with the ionic size and charge of the cation.A widely used cation exchange resin is that obtained by the copolymerization by sulfonating. We may define a cation exchange resin as a high molecular weight cross-linked polymer containing sulfonic group as an integral part of the resin and equivalent amount of cations (Helfferichm, Plesset, 1962). Organically engineered inactive support for the inorganic nanostructured materials has been fabricated where commercial resin has been shown to give some promise. NPs may be stabilized following a few protocols that include:(i)electrostatic stabilization; (ii) steric stabilization and (iii)stabilization by ligand, surfactant, or polymer (Roucouxet al., 2002).Among these synthesis methods, dispersions of metallic NPs by chemicalmethods such as the reduction of metal salts is the most convenient way to control the size of the particles in case of Fe &Mn NPs on PU. C-145 resin and AM IR 120 H resin, respectively(Matthewet al., 2003, Cumbal,Sengupta, 2005). However, immobilization of $[Fe(bpy)_3]^{2+}$ on astrongly acidic cation Exchanger (AM. IR 120 H resin) or in situ formation of the same cationic complex onto a resin matrix (DO.CSA 29 resin) and subsequent modified hydrothermolysis (MHT) at ~ 110^oC produces unusually stable Hierarchical super paramagnetic magnetite Fe_3O_4(BASU et al. 2010). Magnetic Fe oxide NPs may be broadly divided into three main classes: paramagnetic, ferromagnetic and super paramagnetic behavior. Paramagnetic behavior denotes that the magnetic dipoles are oriented in random directions at normal temperatures due to unpaired electrons, which causes a low positive susceptibility (weak interaction) in a magnetic field. Ferromagnetic materials depend on their domain structure to remain magnetized even in the absence of an applied magnetic field but size decreases to less than the domain size when they undergo a significant change. Superparamagnetism tends to have larger magnetic susceptibility than paramagnets since the magnetic moment of the entire nanoparticle aligns in the direction of the magnetic field (Daouet al., 2006, Simeonidiset al., 2007). Therefore, the main objective of this study was to synthesize Fe and Mn NPs using simple Chemicalmethods by the reduction of metal salts and subsequent modified hydrothermolysis (MHT) produces unusually stable HierarchicalSPMM Fe_3O_4. These methods have proven to be the most promising methods for the production of NPs as the procedure is relatively simple and the particles can be obtained with very good controlled particle size, energy saving and eco-friendly process for the production of low-costNPs. To characterize these NPs using SEM, XRD, FTIR and MSB.

Materials and methods:-

Chemicals and Preparations:-

The strong acid cation exchangersDO.CSA 29 resin, PU. C-145and AM. IR 120 H proposed for many water treatment applications, which were used as Resin Supports in this study. The characteristics of these resinsare shown in Table 1. The chemicals and solutions used in this study are of the highest available purity from Sigma–Aldrich analytical grade. The stock solution was further diluted to the required experimental concentration following standard method procedures (APHA, 2005).

Table 1:-Typical Physical and Chemical Characteristics of PU. C-145, DO. CSA29 and AM. IR 120H.

No.	Properties Parameters	PU. C-145	DO. CSA29	AM. - IR 120H
1	Physical form	Spherical beads	Hard Moist Beds	Amber spherical beads
2	Polymer Structure (Matrix)	Macroporous polystyrene crosslinked with divinylbenzene	Corss linked polyStyrene Gel	Styrene divinylbenzene copolymer
3	Functional group	Sulfonic Acid	SO_3 Sulfonic acid	Sulphonates
4	Ionic form as shipped	Na+	H^+ - hydrogen, Na^+-sodium	H^+
5	Total exchange capacity (Min.)	1.5 eq.l^{-1} (32.7 Kgr.ft^{3-1}) (Na+ form)	2.00 (H^+ form), ≥ 2.10 Na^+ form	≥ 1.80 eq.L^{-1} (H^+ form)
6	Moisture holding capacity (Moisture Retention)	55 - 60 % (Na+ form)	43 - 52 % (H+ form), 40 - 45 % (Na+ form)	53 to 58 % (H^+ form)
7	Shipping weight (approx.)	770 - 805 g.l^{-1} (48.1 - 50.3 lb.ft^{3-1})	800-850	800 g.L^{-1}
8	Specific gravity	1.22 (Na^+ form)	----------	1.185 to 1.215 (H^+ form)
9	Uniformity coefficient (max.)	1.7	----------	≤ 1.8
10	Harmonic mean size (Particle Size Range)	300 - 1200 µm	300 - 1200 µm	620 to 830 µm
11	Fine contents	1 % (max.)	----------	< 0.300 mm - 2 % (max.)
12	Max. reversible swelling	$Na^+ \rightarrow H^+$: 6 %	$Na^+ \rightarrow H^+$: 6-8 %	$Na^+ \rightarrow H^+$: 11 %
13	Chemical resistance	Insoluble in dilute solutions of acids or bases and common solvents.	The same	The same
14	pH limits	0 -14	0-14	0-14
15	Max. operating temperature	140°C (285°F)	120 °C	135 °C
16	Application	Demineralization - Highly porous - Na^+ form	Demineralization - Highly porous - Na^+&H^+form	Demineralization - Highly porous - &H^+form
17	Manufacture	PU. Co, USA	DO. Veolia Co. India	Rohm & Haas, French

Synthesis of FeNPs on PU. C-145 Resin Support:-

FeNPs are synthesized using PU. C-145 Resin Support involves following: (i) Loading of Fe(III) onto the sulfonic acid sites of the PU. C-145 by passing 4% FeCl3 solution at an approximate pH of 2.0; (ii) Desorption of Fe(III) and simultaneous precipitation of Fe(III) hydroxides within the gel and pore phase of the exchanger through passage of a solution containing both NaCl and NaOH, each at 5% w/v concentration and (iii)Rinsing and washing with a 50/50 ethanol– water solution followed by a mild thermal treatment (50–60^{o}C) for 60 min. Charged cation exchange resins are immobilized with the cationic metallic solution or with the cationic complex solution. Then the Fe ion charged resin beads are reduced using various reducing agents as the next mechanism (Figure1)(Matthewet al., 2003,Cumbal,Sengupta, 2005).High concentration of sulfonic acid functionalgroups allowed high uniform loading ofHFO particles (approximately 9–12% of Fe by mass) within the polymeric beads. Since, HFO particles residewithin the macropores of the PU. C-145beads.

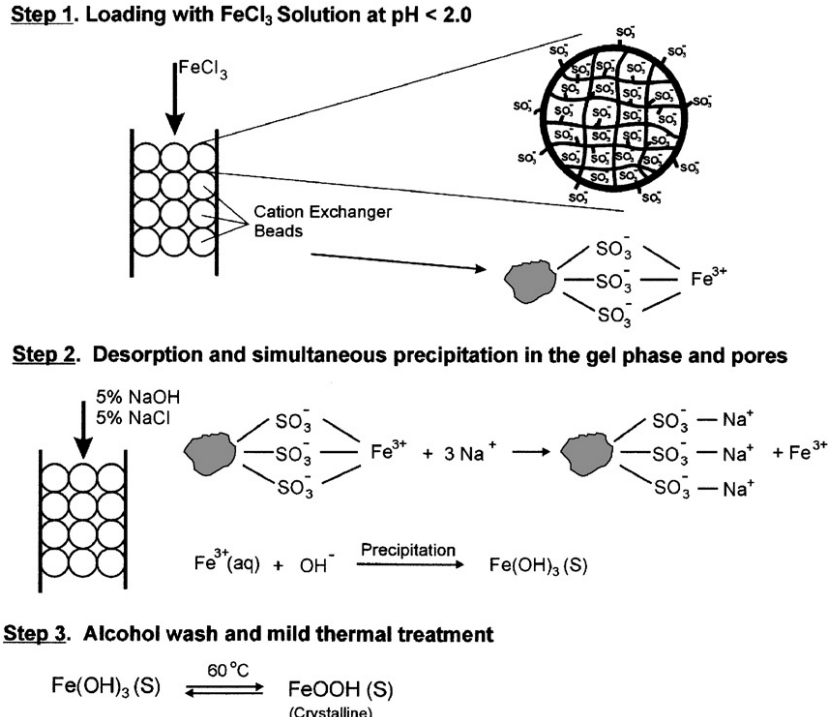

Fig. 1:- Explain of steps procedure to disperse both crystalline and amorphous hydrated Fe oxide (HFO) microparticles inside the spherical PU. C-145 Resin beads.

Synthesis of MnNPs on AM. IR 120 H Resin Support:-

The first step charged AM. IR 120 Hresin is immobilized with the cationic metallic solution. The synthesis of MnNPs on AM. IR 120 H Resin Support was performed by using Mn(II) salts are Mn(II) sulphate involves Loading of Mn(II) from $MnSO_4$ onto the sulfonic acid sites of AM. IR 120 Hexchanger by passing 8 % $MnSO_4$ solution with stirring for 6 hours at an approximate pH of 2.63. Then Desorption of Mn(II) and simultaneous precipitation of Mn(II) oxides within the gel and pore phase of the exchanger through passage of a solution containing NaOHandNaCl, each at 5% w/v concentration. The previous step was repeated for the second time to achieve greaterMn(II) loading After that Rinsing and washing with a 50/50 ethanol– water solution followed by a mild thermal treatment (50–55^oC) for 80 min(Matthewet al., 2003,Cumbal,Sengupta, 2005).

Synthesis of Fe_3O_4NWs on DO.CSA 29 ResinSupport:-

SPMM Fe3O4 NWNPs are synthesized using The brilliant red $[Fe(bpy)_3]^{2+}$ complex upon immobilization on DO.CSA 29 Resin or in situ formation of the same cationic complex onto a resin matrix and subsequent modified hydrothermolysis (MHT) at ~110 °C produces unusually stable hierarchical magnetite Fe_3O_4 NWs. The procedure as the following: At first, DO. CSA 29 Resin was incubated in 0.1M HCl for 12 h to convert all the resin beads to the H form, the washed H forms of the DO.CSA 29 Resin beads were used and 10 ml of laboratory prepared aqueous $[Fe(bpy)_3]^{2+}$ solution was added and stirred for the immobilization. After complete exchange of the cationic complex with the resin matrix, the beads turned red. Then 0.5 g of the red colored resin beads were placed in a screw capped test tube and 5mL of 0.1M solution of NaOH was added and heated under a 100Wbulb at ~100 ^oC for the modified hydrothermolysis (MHT) reaction. After 8 hr. of heat treatment, the red-colored beads became black-coloredFe_3O_4magnetic NWs were obtained as the next scheme(Figure2, 3)(BASU et al., 2010).

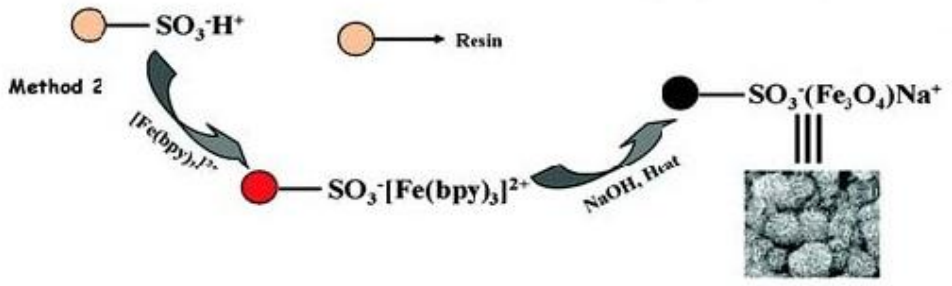

Fig. 2. Formation ofSPMM Fe3O4 NWNPssupport on DO.CSA 29 Resin

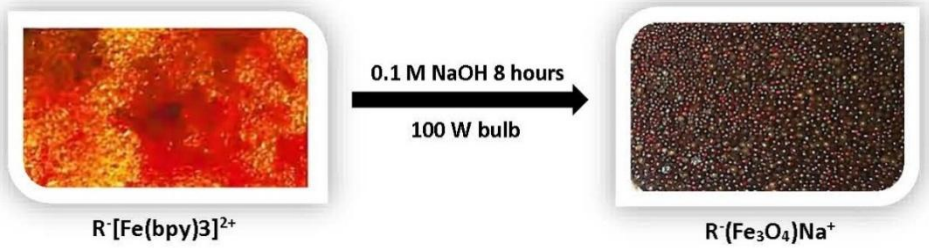

Fig. 3:-Images of the Fe_3O_4 formation and its magnetic nature.

Synthesis of Fe_3O_4NWs on AM. IR I20 H Resin Support:-

The preparation of Fe_3O_4 nanostructure, large wafers were prepared. 1 g of AM. IR I20 H Resinin the H form as the same in previous procedure. Then 100mL of 0.1M NaOH, 100mL of 0.1M aqueous solution of ammonium ferrous sulfate, 100mL of 0.1M alcoholic solution of 2,2´-bipyridine, and 100mL of 0.1M $[Fe(bpy)_3]^{2+}$ were prepared separately at first 10mL of the 0.1M Fe(II) solution, as ammonium ferrous sulfate, was added to 1 g washed AM IR 120 H Resin beads. The mixture was magnetically stirred for uniform immobilization of Fe (II) ions onto the resin beads. After ~ 15 min of stirring, 10mL of fresh aliquot ammonium ferrous sulfate solution was added and stirred. This procedure was continued for the uptake of max. amount of Fe (II) ion by the resin matrix and the resin beads were thoroughly washed with water to remove the unexchanged Fe(II) solution. After that, 30mL of 0.1M aqueous alcoholic solution of 2,2´-bipyridine was added to the Fe(II) immobilized resin beads. The addition of 2,2´-bipyridine solution made the resin beads red in color, indicating the formation of the $[Fe(bpy)3]^{2+}$ complex on the cation exchange resin surface. The red-colored resin beads were washed thoroughly with water and dried inair. Now 0.5 g of the dried resin beads were put into a 15mL screw capped test tube. The screw-capped test tube was partially filled with 5mL of 0.1M solution of NaOH and heated under a 100Wbulb at ~100 ^{o}C for the modified hydrothermolysis (MHT) reaction. After 8 hr. of heat treatment, the red-colored beads became black (Figure3) as the next scheme(Figure4)(Basuet al., 2010).

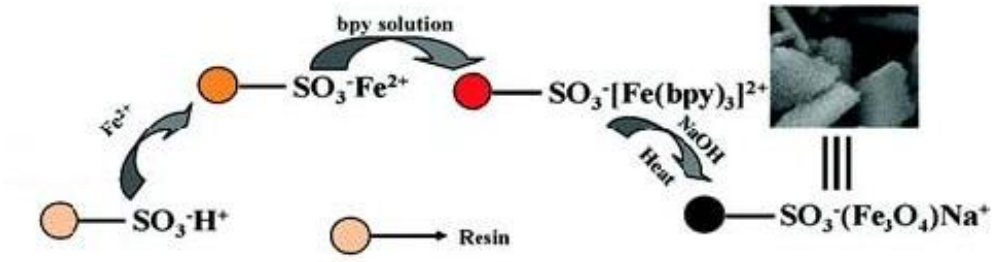

Fig. 4:-Formation ofSPMM Fe_3O_4 NWs support on AM. IRI 20 H Resin.

Characterization Technique:-

SEM using a Joel scanning microscope model JSM5410 determined the properties of formed Fe NPs, Mn NPs and SPMM Fe_3O_4 NWNPs. Sample was deposited on a sample holder with an adhesive carbon foil and sputtered with

gold XRDdata were collected between 1° < 2θ < 80°using a Brukeraxs, D8 advance. The patterns were run with Ni-filtered copper radiation (λ=0.1541 nm) at 30 kV and 10 m A with a scanning speed of 2Θ = 2.5° min^{-1}, FTIR (FT/IR-4100typeA, S. No. B154461016) in the wavelength range 449.333-4000.6 cm^{-1} and MSB using Sherwood Scientific , England, Model-MSB1and S. No. MSB1/230/95/6801 for SPMM Fe_3O_4 NWNPs to get the effective magnetic moment (μ_{eff}).

Results and Discussion:

The synthesized Fe &Mn and SPMM Fe_3O_4 NWNPs were run on SEM,XRD and FTIR , MSB and Characterization of morphology, pores and size, strong magnetic of magnetite for NPswere confirmed as the following:

Characteristics of FeNPs:

SEMofFe NPs:-

Figure5(A) shows a photograph of spherical beads; note that the spherical geometry is retained after processing. Figure 5(B) shows SEM a sliced PU. C-145 particle; both crystalline and amorphous hydrated Fe oxide (HFO)NPs are present on the interior surface. SEM image of Fe-particle at low resolution reveals the dispersion of Fe-particle with relatively less uniformity and low size range 100-350nm as well. A series of SEM pictures taken for PU. C-145 particles and close physical observation suggest that HFO agglomerates are accessible to dissolved solutes through a network of pores(Sengupta et al., 2003).

Fig. 5:-(A) Photo of Fe NPs support on PU. C-145 Resin beads

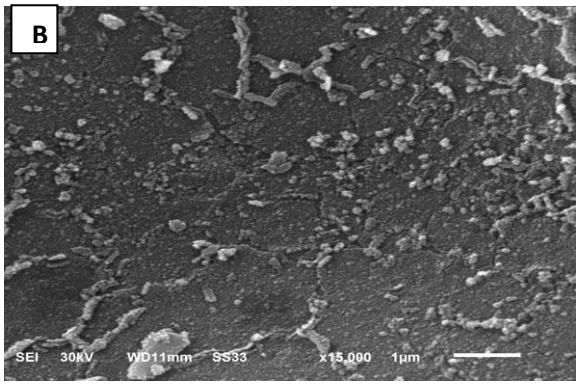

Fig 5:-(B) SEM (15,000X) of a sliced Fe NPs bead.

XRDof Fe NPs:-

The detailsXRD patterns of the Fe NPsare shown in Figure 6.All the reflection peaks with relative intensities of different planes, indexed in the figure, specify the presence of $Fe(OH)_3$. The well crystalline nature of the prepared sample is easily being observed with the sharpness and the intensity of the peaks. noticeable diffraction lines at 2Θ = 10.2, 11.97, 13.17, 21.2, 25.11, 38.97, 51.88, 55.13, and 68.93° which indicates the crystalline phase$Fe(OH)_3$.From XRD pattern, it is clear that Fe NPs synthesized were purely crystalline in nature.Average particle size of Mn oxide NPs was found to be 2.30 to 6.60 nm. Size of $Fe(OH)_3$NPs corresponding to 100 percent intensity peak correspond to 62 as calculated using Scherrer equation$\{D= K\lambda / (\beta COS \Theta)\}$(Leroy, Harold 1950, Ahmad, 2012).

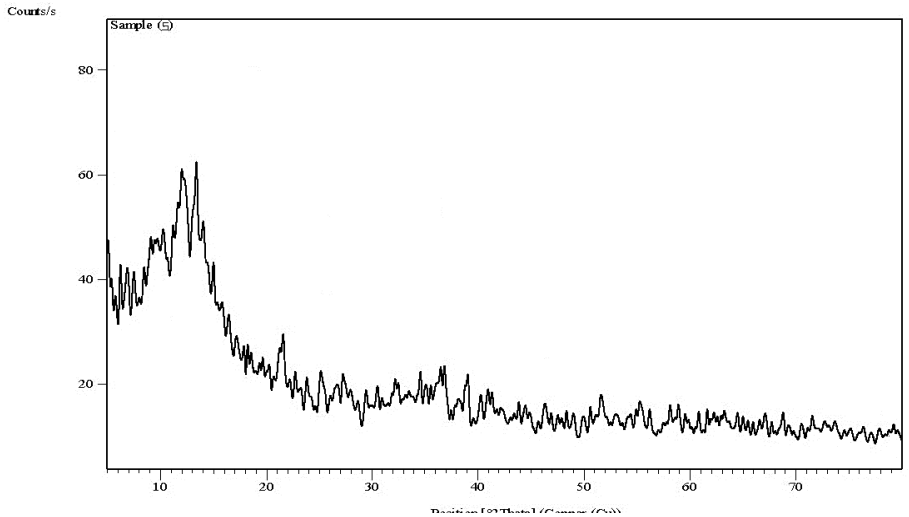

Fig. 6:-XRD pattern of Fe NPs.

FTIR of Fe NPs:-

Figure7shows FTIR spectra of Fe NPs synthesized which was carried out in order to ascertain the purity and nature of Fe NPs. Oxides and hydroxides of metal NPs generally gives absorption peak in the finger print region i.e. below wavelength of 1000 nm arising from inter-atomic vibrations. FTIR spectrum of $Fe(OH)_3$ is represents four absorption bands at around 578.54, 676.785,774.279 and 835.99 cm^{-1} which is due to the presence of Fe-O bond of $Fe(OH)_3$ (Figure 7). Absorption peak observed at 3451.96 cm^{-1}may be due to -CH3 stretching vibrations. The absorption peaks at 2925.48 cm^{-1}, 2362.37 cm^{-1}, 1638.23 $cm^{-1}$and 1415.49 may be due to –CH2 stretching, =C-H stretching and –C-H stretching vibrations. Peaks appeared at 1191.79 cm^{-1}, 1128.15 cm^{-1} and 1040.41 cm^{-1} is due to C-O stretching showing the absorption of atmospheric water and CO_2.

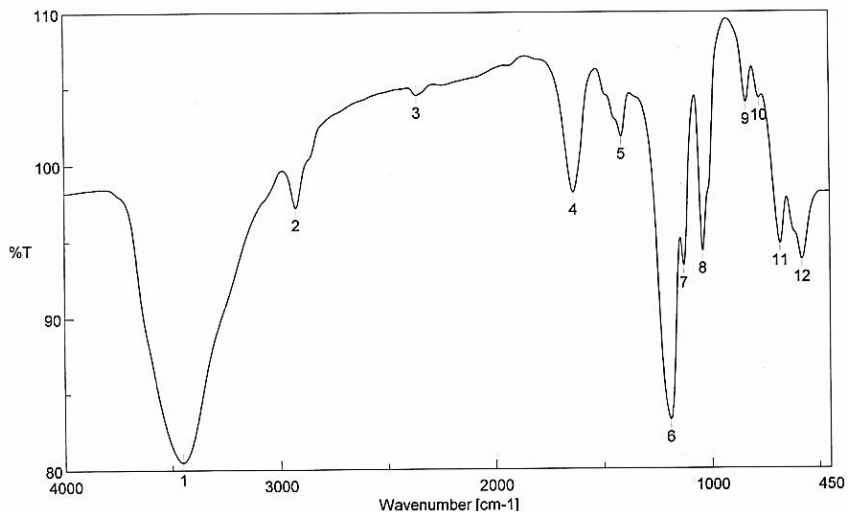

Fig 7:-FTIR spectra of ofFe NPs.

Characteristics of Mn NPs:-

SEMofMn NPs:-

Figure 8(A) shows a photograph of spherical beads. Figure8 (B) shows SEM a slicedAM IR 120 H Resin particle; both crystalline and Mn oxide metal (MnO)NPs are present on the interior surface. SEMimage of Mn_3O_4nanoparticle at low resolution reveals the dispersion of Mn-particle with relatively less uniformity and low size range 100-300 nm as well. A series of SEM pictures taken for AM.IR I20 H particles and close physical observation suggest that MnO agglomerates are accessible to dissolved solutes through a network of pores (Sengupta et al., 2003).

Fig. 8:- (A) Photo of Mn NPs support on AM. IR I20 H Resin beads

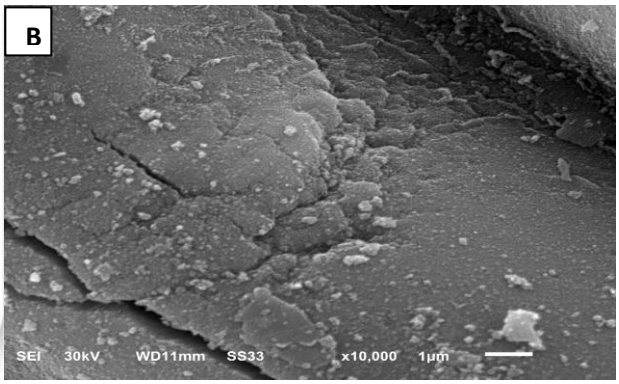

Fig. 8:- (B) SEM (10,000X) of a sliced Mn NPs bead.

XRD ofMn NPs:-

XRD patterns of the Mn NPsare shown in Figure 9. All the reflection peaks specify the presence of Mn_3O_4. The well crystalline nature of the prepared sample is easily being observed with the sharpness and the intensity of the peaks. Noticeable diffraction lines at 2Ɵ = 18.14, 28.84, 31.2, 32.55, 36.22, 38.28, 44.38, 49.66, 59.94, 64.66and 76.6°which indicates the crystalline phase Mn_3O_4. From XRD pattern, it is clear that Mn NPs synthesized were purely crystalline in nature. Average particle size of Mn oxide NPs was foundto be 2.60 to 65.70 nm. Size of Mn_3O_4NPs corresponding to 100 percent intensity peak correspond to 41.52.

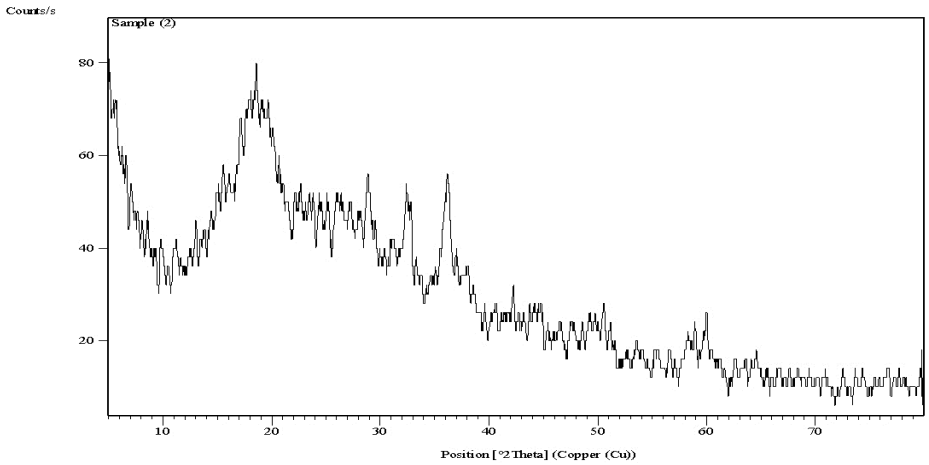

Fig. 9:-XRD pattern of Mn oxide metal NPs.

FTIR of Mn NPs:-

Figure 10 shows FTIR spectra of Mn NPs synthesized. FTIR spectrum of Mn_3O_4 is represents five absorption bands at around 582.397, 615.181, 677.856, 777.172 and 835.026cm^{-1} which is due to the presence of Mn-O bond of Mn_3O_4(Figure10). Absorption peaks observed at 3863.68 and3444.24cm^{-1}may be due to -CH3 stretching vibrations. The absorption peaks at 2922.59cm^{-1}, 1636.3, 1488.24, 1447.31 and 1413.57 may be due to –CH2 stretching, =C-H stretching and –C-H stretching vibrations. Peaks appeared at 1186.01, 1124.3, 1039.44and 1005.7 cm^{-1} is due to C-O stretching showing the absorption of atmospheric water and CO_2.

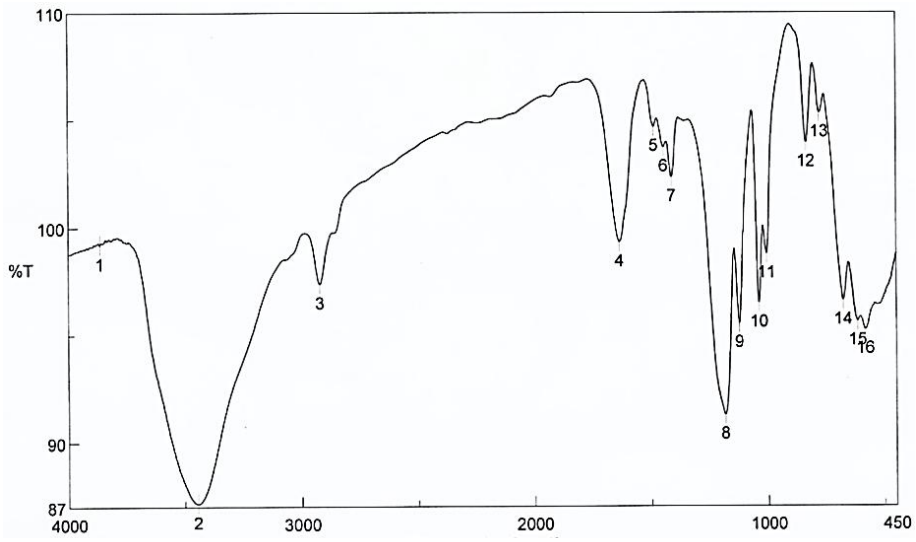

Fig. 10:- FTIR spectra of Mn oxide metal NPs.

Characteristicsof SPMM Fe_3O_4 NWNPs support on DO. CSA 29 Resin:-

SEMof Magnetite Fe_3O_4NPs support on DO. CSA 29 Resin:-

Figure 11(A) shows a photograph of spherical beads. Figure 11(B) shows SEMa sliced DO. CSA 29 particle; both crystalline and Magnetite Fe_3O_4NPs are present on the interior surface. SEMimage of Fe oxide particle at low resolution reveals the dispersion of Fe_3O_4 particle with relatively less uniformity and low size range 100-200 nm as well. A series of SEM pictures taken for DO. CSA 29 particles and close physical observation suggest that Fe_3O_4 agglomerates are accessible to dissolved solutes through a network of pores(Basu et al., 2010).

Fig. 11:- (A) Photo of SPMM Fe_3O_4 NWNPs support on DO. CSA 29 Resin beads.

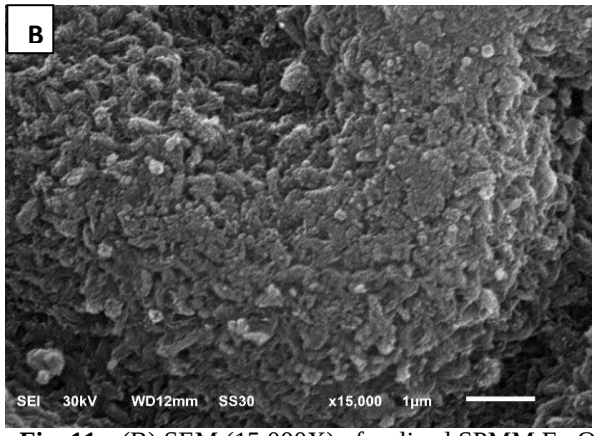

Fig. 11:- (B) SEM (15,000X) of a sliced SPMM Fe_3O_4 NWNPs bead.

XRD of Magnetite Fe_3O_4 NPs support on DO. CSA 29 Resin:-

The detailsXRD patterns of the Fe_3O_4 NPsare shown in Figure 12. All the reflection peaks specify the presence of Fe_3O_4. The well crystalline nature of the prepared sample is easily being observed with the sharpness and the intensity of the peaks. Noticeable diffraction lines at 2Θ = 17.75, 30.2, 35.48, 37.14, 47.31, 53.62, 53.76, 58.27, 62.57, 62.91, 65.8. 71 and 74.35°, which indicates the crystalline phase MagnetiteFe oxide (Fe_3O_4.). From XRD pattern, it is clear thatFe_3O_4NPs synthesized were purely crystalline in nature. Average particle size of Magnetite Fe oxide Fe_3O_4 NPswas found to be 16.0 to 56.50nm. Size of Fe_3O_4 NPs corresponding to 100 percent intensity peakcorrespond to 100.

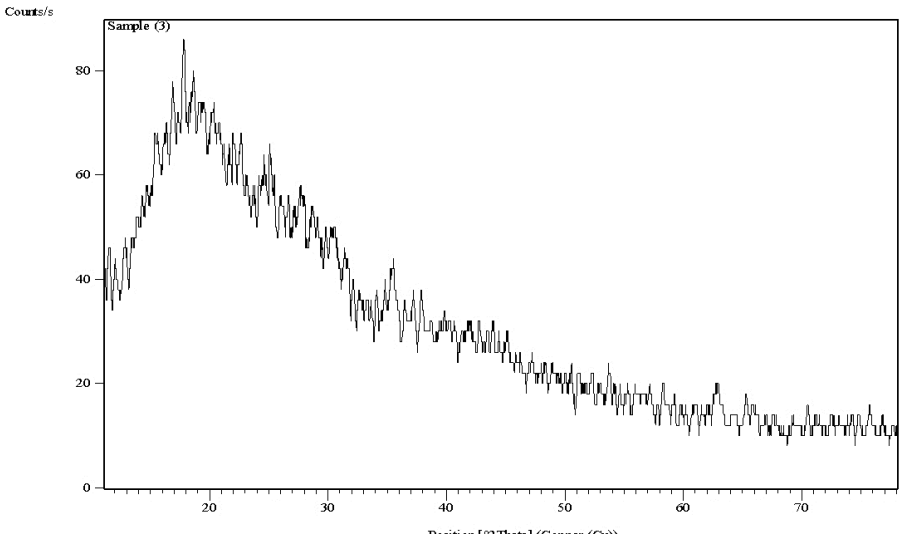

Fig. 12:-XRD pattern of MagnetiteFe_3O_4NPssupport on DO.CSA 29 Resin.

FTIRof Magnetite Fe_3O_4 NPs support on DO. CSA 29 Resin:-

Figure 13 shows FTIR spectra of Fe_3O_4 NPs synthesized. FTIR spectrum of Fe_3O_4 is represents four absorption bands at around 574.683, 677.856,774.279 and 835.026 cm^{-1} which is due to the presence of Fe-O bond of Fe_3O_4 (Figure 13). Absorption peak observed at 3443.28cm^{-1}may be due to -CH3 stretching vibrations. The absorption peaks at 2925.48, 1636.3 and 1415.49 may be due to –CH2 stretching, =C-H stretching and –C-H stretching vibrations. Peaks appeared at 1181.19, 1125.26, 1034.62 and 1007.62 cm^{-1} is due to C-O stretching showing the absorption of atmospheric water and CO_2.

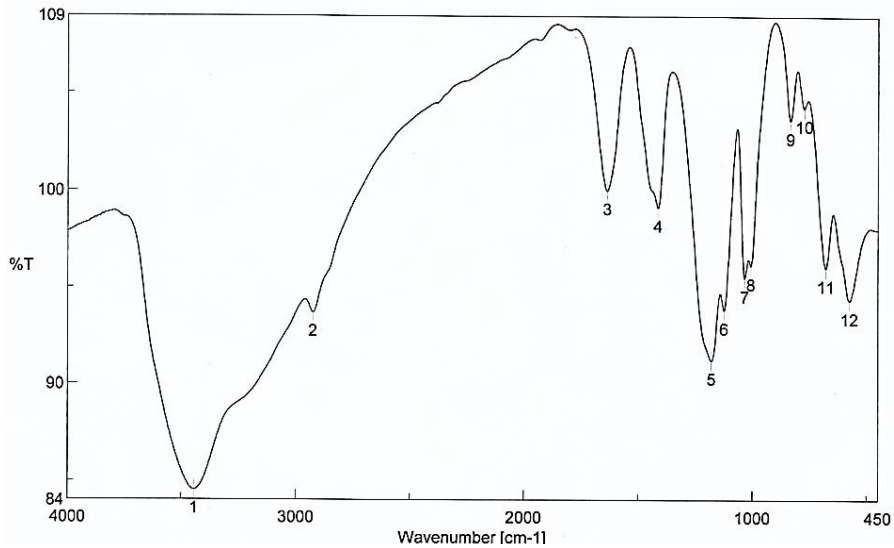

Fig. 13:-FTIR spectra of of Magnetite Fe_3O_4 NPssupport on DO. CSA 29 Resin

Magnetic Susceptibility Measurement for of Magnetite Fe_3O_4 NPs support on DO. CSA 29 Resin:-

The mass susceptibility, χg, is calculated from the equation:

$$\chi_g = \{C_{Bal} .L.(R-R_o)\}/\{(m - m_o) x10^9\}$$

Where L= sample length (cm); m - m_o = sample mass (g); R = reading for tube + sample; R_o = reading for empty tube; C_{Bal} = the balance calibration constant written on the back of the instrument (C_{Bal} = 2.086). This incorporates the area cross-section of the sample tube. The analysis data areshown in table 2:

Table 2:-The analysis data of Magnetite Fe_3O_4 NPs support on DO. CSA 29 Resin requirement to calculate of the effective magnetic moment

m_o (gm)	m (gm)	m - m_o (gm)	L (cm)	Ro Empty	R sample	R-Ro	C_{Bal}	M.wt of Complex g.mol^{-1}
0.672	0.859	0.187	2.6	- 30	1835 x 10	1838 x 10	2.086	438.693

$$\chi_g = 5.331 \times 10^{-4} \text{ emu.gm}^{-1}$$

Now χg is the magnetic susceptibility per gram and must be a positive number. If R> R_o then diamagnetism is indicated. To convert this to the molar susceptibility, multiplyχ_g* molecular weight. Because ligands and the central metal will contribute a negative effect because of theirdiamagnetism, the magnetic susceptibility for the complex (Magnetite Fe_3O_4Nanowaferssupport on DO. CSA 29 Resin) can be found by adding thediamagnetic contributions of the ligands and the metal to χm. This gives χ_A

$$\chi_m = \chi g \times M.wt, \quad \text{Then} \quad \chi_m = 438.693 \times 5.331 \times 10^{-4}$$
$$\chi_A = 0.234$$

M.Wt = molecular weight of complex (Magnetite Fe_3O_4 NWs support on DO. CSA 29 Resin), the effective magnetic moment, $\mu_{eff}$is given by $\mu_{eff} = \sqrt{[\{3.k.T.\chi_A\}/\{N.B^2\}]}$

Where N = Avogadro's number; B = the Bohr magneton; k = Boltzmann's constant; T = absolutetemperature.Combining the constants reduces the formula to

$$\mu_{eff} = 2.828\sqrt{(\chi_A T)}, \quad \text{Then} \quad \mu_{eff} = 23.62 \text{ emu.mol}^{-1}$$

The effective magnetic moment of super paramagnetic magnetite Fe_3O_4Nanowafers=**23.62emu.mol^{-1}**

Characteristics of SPMM Fe_3O_4 NWNPs on AM. IR 120 H Resin support:-

SEM for of Magnetite Fe_3O_4 NPs support on AM.IR I20 H Resin:-

Figure 14(A) shows a photograph of spherical beads. Figure 14(B) shows SEMa sliced AM.IR I20 H particle; both crystalline and Magnetite Fe_3O_4 NPs are present on the interior surface. SEMimage of Fe oxide particle at low resolution reveals the dispersion of Fe_3O_4 particle with relatively less uniformity and low size range 100-200 nm as well. A series of SEM pictures taken for AM. IR I20 H particles and close physical observation suggest that Fe_3O_4 agglomerates are accessible to dissolved solutes through a network of pores (Basu et al., 2010).

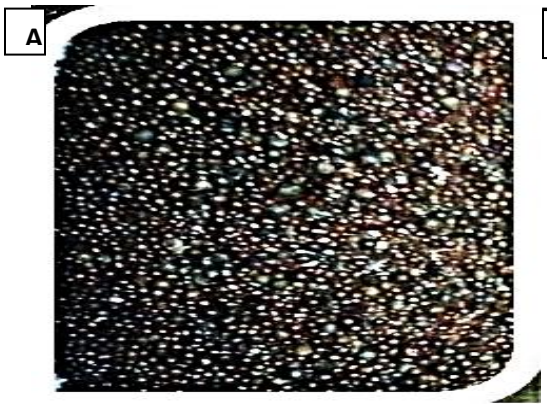

Fig. 14:- (A) Photo of SPMM Fe_3O_4 NWNPs support on AM. IR I20 H Resin beads

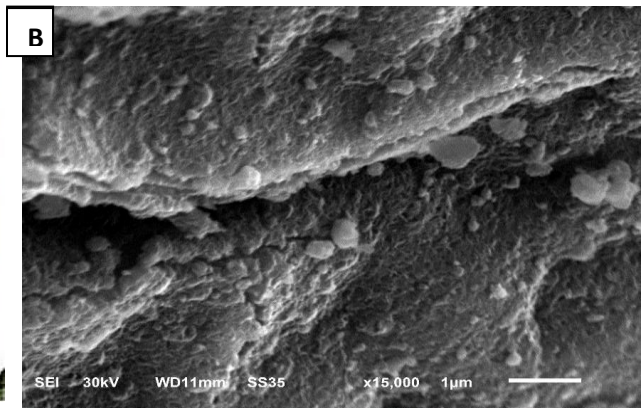

Fig. 14:- (B) SEM (15,000X) of a sliced SPMM Fe_3O_4 NWNPs bead.

XRD ofMagnetite Fe_3O_4 NPs support on AM.IR I20 H Resin:-

The detailsXRD patterns of the Fe_3O_4 NPsare shown in Figure 15. All the reflection peaks specify the presence of Fe_3O_4. The well crystalline nature of the prepared sample is easily being observed with the sharpness and the intensity of the peaks. noticeable diffraction lines at 2Θ = 18.14, 35.43, 43.1, 53.24, 57.1 and 62.76°which indicates the crystalline phase Magnetite Fe oxide Fe_3O_4.From XRD pattern, it is clear that Fe_3O_4 NPs synthesized were purely crystalline in nature. Average particle size of Magnetite Fe oxide Fe_3O_4NPs was found to be 2.90 to 33.20 nm. Size of Fe_3O_4 NPs corresponding to 100 percent intensity peak correspond to 100.

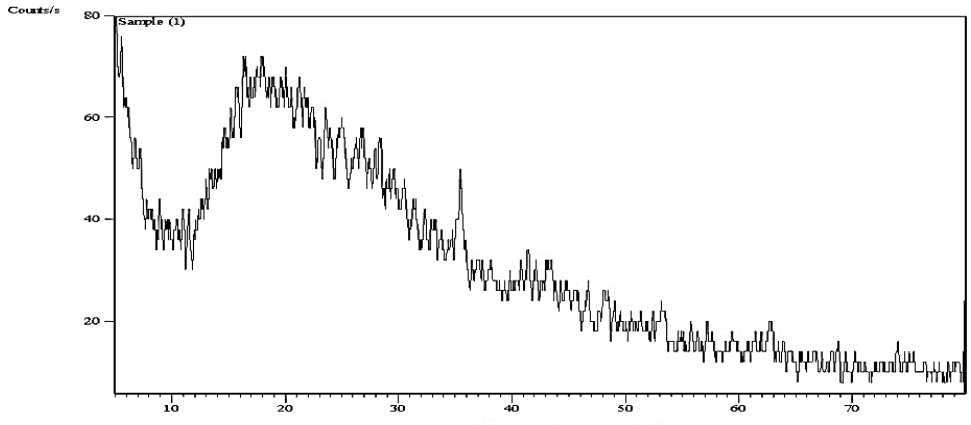

Fig. 15:-XRD pattern of MagnetiteFe_3O_4NPssupport on AM. IR I20 H Resin.

FTIR of Magnetite Fe_3O_4 NPs support on AM.IRI 20 H Resin:-

Figure 16 shows FTIR spectra of Fe_3O_4 NPs synthesized. FTIR spectrum of Fe_3O_4 is represents four absorption bands at around 575.647, 675.928,775.244 and 835.026 cm^{-1} which is due to the presence of Fe-O bond of Fe_3O_4 (Figure 16). Absorption peak observed at 3442.31cm^{-1}may be due to -CH3 stretching vibrations. The absorption peaks at 2924.52, 2363.34, 1636.3, 1447.31 and 1415.49 cm^{-1}may be due to –CH2 stretching, =C-H stretching and –C-H stretching vibrations. Peaks appeared at 1177.33, 1122.37, 1036.55 and 1002.8 cm^{-1} is due to C-O stretching showing the absorption of atmospheric water and CO_2.

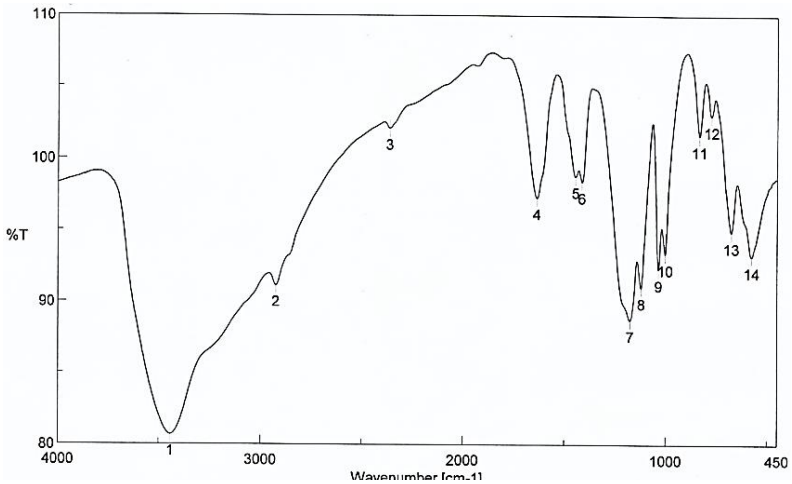

Fig. 16:- FTIR spectra of of MagnetiteFe_3O_4NPssupport on AM. IR I20 H Resin.

Magnetic Susceptibility Measurement for of Magnetite Fe_3O_4 NPs support on AM. IR I20 H Resin:-

The mass susceptibility, χg, is calculated from the equation:

$$\chi_g = \{C_{Bal} .L.(R-R_o)\}/\{(m - m_o) x10^9\}$$

The analysis data areshown in table 3:

Table 3:-The analysis data of Magnetite Fe_3O_4 NPs support on AM. IR I20 H Resin requirement to calculate of the effective magnetic moment.

m_o (gm)	m (gm)	$m - m_o$ (gm)	L (cm)	Ro Empty	R sample	R-Ro	C_{Bal}	M.wt of Complex $g.mol^{-1}$
0.672	0.811	0.139	1.8	- 30	1835 x 10	1833 x 10	2.086	829.30452

$$\chi_g = 4.96 \times 10^{-4} \text{ emu.gm}^{-1}$$

The magnetic susceptibility for the complex (Magnetite Fe_3O_4NWssupport on AM. IR I20 H Resin) can be found by adding thediamagnetic contributions of the ligands and the metal to χm. This gives χ_A

$$\chi_m = \chi g \times M.wt\ , \qquad \text{Then} \quad \chi_m = 829.30452 \times 4.96 \times 10^{-4}$$

$$\chi_A = 0.4113$$

M.wt = molecular weight of complex (Magnetite Fe_3O_4NWssupport on AM.IR I20 H Resin), the effective magnetic moment, $\mu_{eff}$is given by $\mu_{eff} = \sqrt{[\{3.k.T.\chi_A\}/\{N.B^2\}]}$

Combining the constants reduces the formula to

$$\mu_{eff} = 2.828\sqrt{(\chi_A T)}\ , \qquad \text{Then} \mu_{eff} = 31.31\ emu.mol^{-1}$$

The effective magnetic moment of super paramagnetic magnetite Fe_3O_4Nanowafers=31.31emu.mol^{-1}

Comparison of the characterizations of synthesized NPsare shown in Table 4.

Table 4:-Comparison of the characterizations of Fe,Mn andSPMM Fe_3O_4 NWNPs.

No.	Characterizations	Fe NPs	Mn NPs	SPMM Fe_3O_4 NWs (DO. CSA 29)	SPMM Fe_3O_4 NWs (AM. IR 120 H)
1	Technique of synthesis	Very simple	Very simple	Simple	Simple
2	Yield	High/scalable	High/scalable	High/scalable	High/scalable
3	SEM (Shape control)	Very good	Very good	Excellent	Excellent
4	XRD	Specify the presence of $Fe(OH)_3$	Specify the presence of Mn_3O_4	Specify the presence of Fe_3O_4	Specify the presence of Fe_3O_4
5	Size Distribution	Very narrow	Relatively narrow	Relatively narrow	Very narrow
6	Size Control average (nm)	2.3-6.6	2.6-65.5	16-56.5	2.9-33.2
7	FTIR	Spectrum of $Fe(OH)_3$ is represents four absorption bands	Spectrum of Mn_3O_4 is represents five absorption bands	Fe_3O_4 is represents four absorption bands	Fe_3O_4 is represents four absorption bands
8	Magnetization property of SPMM Fe_3O_4	----------	----------	μ_{eff} = 23.62 emu.mol^{-1}	μ_{eff} = 31.31 emu.mol^{-1}

Therefore, we are made descending arrangement for these synthesizedNPs according to results percentage of perfect charactersare shown in table 5 and figure 17 as the next: 1- SPMM Fe_3O_4NWs (AM. IR 120 H), 2- SPMM Fe_3O_4 NWs (DO. CSA 29), 3- Fe NPs, 4- Mn NPs.

Table 5:-Comparison of percentage of perfect charactersof Fe,Mn andSPMM Fe_3O_4 NWNPs.

No.	Characterizations	Iron Nanoparticles	Manganese Nanoparticles	SPMM Fe3O4 Nanowafers (DOSHION CSA 29)	SPMM Fe_3O_4Nanowafers (AMBERLITE IR 120 H)
1	Technique of synthesis	100%	100%	75%	75%
2	Yield	100%	100%	100%	100%
3	SEM (Shape control)	75%	75%	100%	100%
4	XRD	100%	100%	100%	100%
5	Size Distribution	100%	75%	75%	100%
6	Size Control average (nm)	100%	50%	50%	75%
7	FTIR	75%	100%	75%	75%
8	Magnetization property of Fe_3O_4	--------	--------	100%	100%

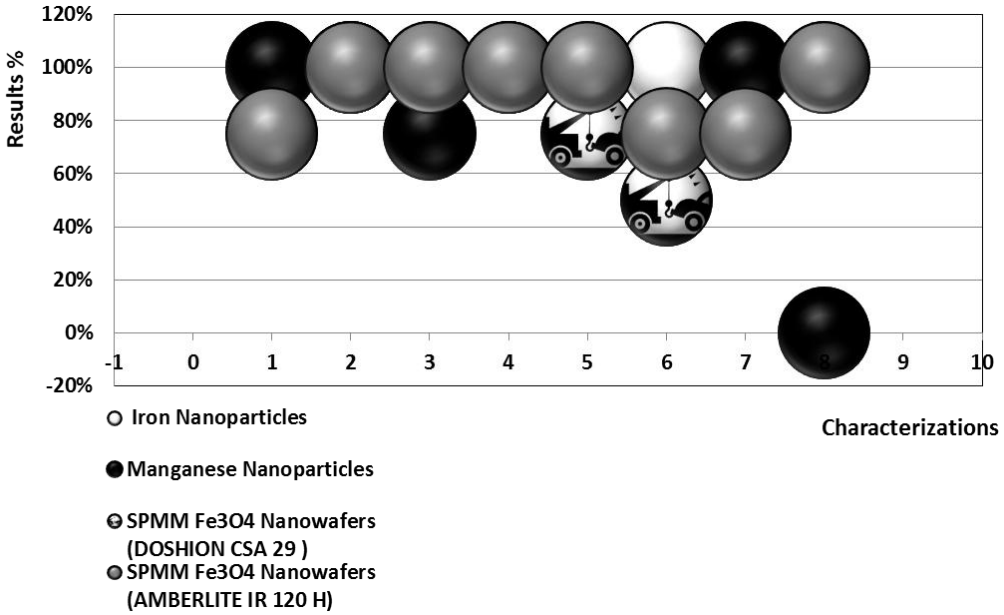

Fig. 17:-Explain the perfect characters of descending arrangement for synthesized NPs.

Conclusions:-

Fe,MnandSPMM Fe_3O_4 NWs NPsare synthesized with particle size ranging between 2.3-6.6 nm, 2.6-65.5 nm,16-56.5 nm and 2.9-33.2 nm (<100nm)respectively,The shape, porous and size of these NPs were confirmed using SEM, XRD and FTIR. The magnetization property of super paramagnetic magnetite Fe_3O_4 (DO. CSA 29) and (AM. IR 120 H)were confirmed using MSB to give the effective magnetic moment (μ_{eff}) wich equal 23.62, 31.31 $emu.mol^{-1}$.Successful exploitation of metallic NPs lies in the successful conjugation of their active surface structure. Thus, size and shape play a role in terms of variable surface energy. The descending arrangement for these synthesized NPs according to results percentage of perfect characters as the next: 1.SPMM Fe_3O_4 NWs(AM. IR 120 H);2. SPMM Fe_3O_4 NWs (DO. CSA 29);3. Fe NPs and 4. Mn NPs.These synthesizedNPshave unique properties and inexpensive materials may be make it possible to envision a series of incomplete removal of hazardous pollutants in industrial wastewater.

References:-

1. Ahmad M., Mohammad R. F., Mohammad R. M.2012. *Modified Scherrer Equation to Estimate More Accurately Nano-Crystallite Size Using XRD*. World Journal of Nano Science and Engineering, 2: 154-160.
2. Aitken Rj, Creely Ks, Tran Cl. 2004. NPs: *An Occupational Hygiene Review, Institute of Occupational Medicine*. Health and Safety Executive (HSE), UK, Research Report, 274: 113.
3. Alagarasi A.2013.*Introduction to nanomaterials.* Rearchgate, 1: 76. https//www. Researchgate.Net/publication/259118068_chapter_INTRODUCTION_TO_NANOMATERIALS
4. Alexandre M., Dubois P.2000. *Polymer-layered silicate nanocomposites: Preparation, properties and uses of a new class of materials.* Mater. Sci. Eng. R., 28:1-63.
5. APHA (American Public Health Association) 2005. *Standard methods for the examination of water and wastewater.* Washington, DC. 21.
6. Aymonier C., Bortzmeyer D., Thomann R., MülhauptR. 2003.Poly (methyl methacrylate)/palladium nanocomposites: *synthesis and characterization of the morphological, thermomechanical and thermal properties.* Chem. Mater., 15: 4874-4878.
7. Basu M., Sinha K., Sarkar S., Pradhan M., Yusuf M., Negishi Y., Pal T. 2010.*Hierarchical superparamagnetic magnetite NWs from a resin-bound* $[Fe(bpy)_3]^{2+}$ *matrix.* Langmuir, 26: 5836.
8. BSI (British Standards International) 2005. Vocabulary NPs. PAS 71: 26.Bureau of National Affairs.2004. *Nanotechnology*. Washington D.C. Conference Report, 34(42):1068-1071.
9. Chauhan. B. P. S. 2011. *Hybrid Nanomaterials: Synthesis, Characterization, and Applications*, John Wiley & Sons, Inc., HOBOKEN, New Jersey. In Canada,1: 27-28.ISBN: 978-0-470-48760-0

10. Cumbal L., SenguptaA. 2005. *Arsenic removal using polymer Supported Hydrated Fe (III) Oxide NPs: Role of Donnan Membrane Effect.*EnvFe. Sci.Technol. 39(17): 6508-6515. DOI: 10. 1021/es050175e
11. Daout.,Pourroy G., B´Egin-Colin S.2006.*Hydrothermal synthesis of monodisperse magnetite NPs*. Chemistry of Materials, 18(18): 4399–4404.
12. El-Moselhy M., Mahmoud N., Emara M. 2014.*Copper modified exchanger for the photodegradation of methyl orange dye*. Journal of Desalination and water treatment, 52(37-39): 7225-7234. DOI: 10.1080/19443994.2013.823625
13. Emara M., El-Moselhy M., Farahat N. 2010. *Photocatalytic degradation of hydroquinone using HFO supported polymeric material*. Journal of Desalination and water treatment, 19(1-3): 232-240. DOI**:**10.5004/dwt.2010.1146
14. Emara M., Tourky S., El-Moselhy M., FarahatN. 2010. *Structural modification of mordenitezeolute with Fe photo-degradation of EDTA*. Journal of Hazardous Materials, 166(1): 514–522. DOI: 10.1016/j.jhazmat.2008.11.044
15. Gogotsi Y. 2006. *Nanomaterials Handbook.* CRC Press,Taylor& Francis Group ,6000 Broken Sound Parkway NW, Suite 300 ,Boca Raton,1: 13-24, FL: 33487-2742. ISBN: 0-8493-2308-8
16. Gyoo P., Venkataramani S., Kim S. 2006. *Morphology thermal and mechanical properties of polyamide 66/clay nanocomposites with epoxy-modified organoclay*. J. Appl. Polym. Sci., 101: 1711-1722.
17. Helfferich F., Plessetm. 1962. *Ion Exchange*. McGraw Hill, New York.Science, 138(3537): 624.
18. ICON (International Councilon Nanotechnology) 2008. Towards Predicting Nano-Biointeractions: *An International Assessment of Nanotechnology*,EnvFement. Health and Safety Research Needs, 4: 80.
19. In-Yup J., Jong-Beom B. 2010. *Nanocomposites Derived from Polymers and Inorganic NPs. Materials*, 3: 3654-3674.DOI: 10.3390/ma3063654
20. Kickelbick G. 2003. *Concepts for the incorporation of inorganic building blocks into organic polymers on a nanoscale*. Prog. Polym. Sci., 28: 83-114.
21. Leroy Al., Harold P. 1950. *Determination of Crystallite Size with the X-Ray*.Journal of Applied Physics. 21: 137.DOI: 10.1063/1.1699612 Spectrometer
22. Matthew J., Sengupta A., Greenleaf J. 2003. *Arsenic removal using a polymeric / inorganic hybrid sorbent*. Water Research, 37(1): 164-176. DOI: 10.1016/S0043-1354(02)002.
23. Okamoto M., Morita S., Kim Y., Kotaka T., TateyamaH. 2000.*Synthesis and structure of sematic clay/poly (methyl methacrylate) and clay/polystyrene nanocomposites via in situ intercalative polymerization*. Polymer, 41: 3887-3890.
24. Roucoux A., Schulz J., Patin H. 2002. *Reduced transition metal colloids: anovel family of reusable catalysts.* [PubMed], Chem. Rev., 102(10): 3757-78.
25. Simeonidis K., Mourdikoudis S., Moulla M. 2007. *Controlled synthesis and phase characterization of Fe-based NPs obtained by thermal decomposition. Journal of Magnetism and Magnetic Materials*, 316(2): e1–e4.
26. Tomasko D., Han X., Liu D., GaoW. 2003. *Supercritical fluid applications in polymer nanocomposites.*Curr. Opin. Solid St. Mater. Sci., 7: 407-412.
27. Vaia R., Giannelis E.1997. *Lattice model of polymer melt intercalation in organically - modified layered silicates*. Macromolecules, 30: 7990-7999.